IEEE Photonics Journal
An IEEE Photonics Society Publication

Open Access

UHD Video Transmission Over Bidirectional Underwater Wireless Optical Communication

Volume 10, Number 2, April 2018

Abdullah Al-Halafi, ***Member, IEEE***
Basem Shihada, ***Senior Member, IEEE***

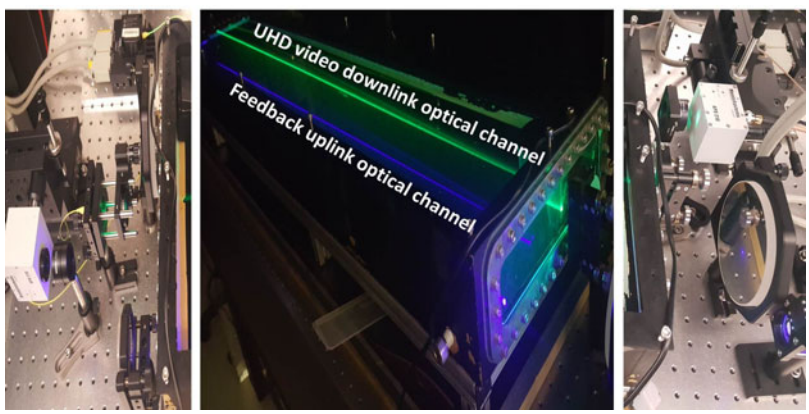

DOI: 10.1109/JPHOT.2018.2821695
1943-0655 © 2018 IEEE

IEEE photonics SOCIETY

IEEE

UHD Video Transmission Over Bidirectional Underwater Wireless Optical Communication

Abdullah Al-Halafi,[1] ***Member, IEEE***,
and Basem Shihada,[1] ***Senior Member, IEEE***

[1]Computer, Electrical and Mathematical Sciences and Engineering Division, King Abdullah University of Science and Technology Thuwal 23955, Saudi Arabia

DOI:10.1109/JPHOT.2018.2821695

Manuscript received March 1, 2018; revised March 24, 2018; accepted March 28, 2018. Date of publication April 2, 2018; date of current version April 11, 2018. Corresponding author: Basem Shihada (e-mail: basem.shihada@kaust.edu.sa).

Abstract: In this paper, we experimentally demonstrate for the first time a bidirectional underwater wireless optical communication system that is capable of transmitting an ultrahigh definition real-time video using a downlink channel while simultaneously receiving the feedback messages on the uplink channel. The links extend up to 4.5 m using QPSK, 16-QAM, and 64-QAM modulations. The system is built using software defined platforms connected to TO-9 packaged pigtailed 520 nm directly modulated green laser diode (LD) with 1.2 GHz bandwidth as the optical transmitter for video streaming on the downlink, and an avalanche photodiode (APD) module as the downlink receiver. The uplink channel is connected to another pigtailed 450 nm directly modulated blue LD with 1.2 GHz bandwidth as the optical uplink transmitter for the feedback channel, and to a second APD as the uplink receiver. We perform laboratory experiments on different water types. The measured throughput is 15 Mb/s for QPSK, and 30 Mb/s for both 16 QAM and 64 QAM. We evaluate the quality of the received live video streams using peak signal-to-noise ratio and achieve values up to 16 dB for 64 QAM when streaming UHD video in harbor II water and 22 dB in clear ocean.

Index Terms: Underwater communication, bi-directional wireless optical communication, ROV, UHD video, diode lasers, QPSK, QAM, OFDM.

1. Introduction

The world population prospects is projected to be 9.7 billion in 2050. It is essential to facilitate monitoring and protecting the existing natural resources, and continuing the discovery for new ones necessary to maintain prosperity and well-being for our future generations [1], [2]. Oceans hold the promise as our final frontier where the untouched depths still remain full of mysteries and natural resources that humans have not been able to reach and uncover so far. Traditionally, marine Remotely Operated Vehicles (ROVs) are used within very limited agility and manipulation abilities to examine and maneuver around the fragile coral reefs and biological specimens. This process can be dangerous, inadequate and harmful to the marine eco-system and deep sea environment if an oil spill accident happens while inspecting or repairing a network of oil and gas subsea pipeline or subsea communication cables [3].

One of the most advanced and latest ROVs is OceanOne [4]. Yet, to make those vehicles more interactive with ocean surroundings, and meet many challenges when accessing oceans deep, it

is imperative to make them fully autonomous when enabled with an ultrafast wireless connections integrated into their robotic intelligence, sensing capabilities, and vision acquisition techniques all together. In order to virtually mimic the human intuition and cognition in real time, and safely perform well in those locations that are unsafe for divers, ROVs must be equipped with state-of-the-art communication technologies that enable underwater real-time video capabilities and provide wireless feedback control links for immediate navigation commands.

Underwater Wireless Optical Communication (UWOC) systems provide the potential for those envisioned underwater vehicles and sensor nodes to gather and send huge amount of information in a short period of time much less than what the current conventional underwater acoustic communications can support [5]. A larger variety of underwater applications such as oceanography and imaging, real-time video streaming, high throughput underwater wireless sensor networks (UWSN) can be exploited using UWOC. Several benefits rely on the high data rates, low latency, and low power consumption that make it more attractive alternative to establish networks between ROVs and UWSN to retrieve, offload, download or exchange larger sets of data in real time while minimizing energy loss and traffic congestions [6].

Recent developments in UWOC systems were demonstrated in several experiments such as in [7]–[11], and achieved up to 16 Gbps where their major themes were to achieve the highest data rate possible. The higher transmission rates are obtained by deploying advanced modulation formats, such as Orthogonal-Frequency-Division-Multiplexing (OFDM), which when implemented together with high-orders of Quadrature-Amplitude-Modulation (QAM) can greatly improve the spectral efficiency of the underwater video transmission system. Moreover, employing QAM-OFDM modulation and directly modulated lasers provides symbol and power efficient loading for different sub-carriers to improve the communication performance. Implementations of OFDM modulation for UWOC experiments have been carried out using either green lasers or blue lasers as in [12], [13]. However, the dominant impairing phenomena of underwater absorption, scattering, and turbulence continue to degrade heavily the performance of underwater video transmission systems [14], [15] and prevent further developments of long range UWOC links.

Throughput rates up to 10 Mbps of underwater video transmission were achieved in previous experiments. In 2005 authors [16] established a 10 Mbps video link based on UWOC system over 4.6 m in clear water. In 2007, experiments in [17] also constructed a 10 Mbps video system over 10 m in Lake water. The AquaOptical II video transmission system [18] used 18 light-emitting diodes (LEDs) with limits of 4 Mbps bandwidth. In addition, authors in [19] demonstrated another video system in a varying water tank visibility. More recently, in an experiment on real-time video streaming using green laser, authors implemented Quadrature-Phase-Shift-Keying (QPSK), and up to 8-QAM modulations in different underwater channels. The work demonstrated that video streaming is possible in one of the most turbid ocean water types, and with good quality [20]. Although those implementations utilized the bandwidths available at that time of deployment, they considered only a single link as a uni-directional communications concept where data streams are sent from a transmitter to a receiver without any feedback on the receiver status, acknowledgements, or channel conditions.

In this work, we implement bi-directional communication links for the purposes of underwater ultra high definition (UHD) and live video streaming on the downlink channel while providing the feedback control messages on the uplink channel. The additional uplink channel provides necessary feedback about the channel conditions, the possibility of using this to transmit and receive control messages, and real-time commands for maneuvering the ROVs. Furthermore, when a wireless optical feedback link is established, movements of multiple robots can be coordinated where the ROVs can move freely and send signaling data and receive further maneuvering instructions in real time. While the feedback for such messages can be established through lower bandwidth acoustic communication links, in a hybrid optical-acoustic configuration, the all-optical links however come in handy if the ROVs form a larger network and start relaying or exchanging real-time videos, or in case the destination becomes in a non-line of sight (NLOS) location. All-optical links are also envisioned to replace the conventional signaling methods used between divers when real-time video can be exchanged from both sides. Moreover, the feedback received on the underwater channel

conditions enables the instantaneous throughput adaptations to the noise levels and transmission power, and thus helps in reducing the energy loss while improving the modulation and coding schemes.

In a nutshell, we experimentally demonstrate the feasibility of the proposed bi-directional system and evaluate its performance under higher orders of QAM implemented with OFDM modulations that enable UHD video transmission in real time. We examine our system by deployments in various underwater channel conditions and analyze the throughput and quality of the received UHD live video streams. The results reveal that UHD video transmission is possible not only in the traditional uni-directional communication setup but also where feedback control messages are established through bi-directional links.

Our main contributions in this work are summarized as follows:

- Design a novel and first of a kind bi-directional system for transmitting real-time and UHD video underwater with feedback using two laser diodes with two distinctive wavelengths for video link and feedback link separately.
- Design an online evaluation algorithm to measure the throughput and attenuation levels at the underwater channel.
- Design an off line evaluation algorithm to measure the quality of the received video when UHD resolution is implemented.
- Implement higher orders of modulations up to 64-QAM-OFDM to enable the transmission of the highest resolution of UHD video, and to achieve the highest throughput records for underwater real-time video applications ever achieved in UWOC systems.
- Demonstrate by laboratory experiments the successful implementation of this integrated system by transmitting and receiving UHD video packets and feedback through the underwater optical channel in real time.
- Evaluate the systems performance using extensive empirical measurements that proof the system's stability under various underwater channel conditions.

The rest of this paper is organized as follows. The proposed system model is presented in Section 2. The experimental setup is described in Section 3. The experimental results and discussions are presented in Section 4. Finally, the paper is concluded in Section 5.

2. System Software Framework

In our model, we integrate the latest LabVIEW software modules into universal software radio peripheral-reconfigurable input/output (USRP-RIO) hardware to transmit live streams of UHD video underwater. We use two USRP-RIO devices operating as Client/Server model. The system's software block diagram is shown in Fig. 1. We will show next the transmitter and receiver software modules for both the downlink and uplink bi-directional configuration.

2.1 Downlink Transmitter Module

In the downlink, the video data are first read from a User Datagram Protocol (UDP) socket into the (Server) when provided by an external application using the (UDP read) command. The video payload is fed into the transport block (TB) in the Field-Programmable Gate Array (FPGA) where medium access control (MAC) layer (MAC TX) implementation will add a header with the number of video payload bytes to the TB, followed by the video bytes and ending with padding. The TB data will be encoded and modulated as a downlink (DL) signal and will be sent by the DL transmitter denoted as (PHY downlink TX).

This physical layer of the downlink transmitter will also encode the Physical Downlink Control Channel (PDCCH), and the Physical Downlink Data Shared Channel (PDSCH). Also, create the downlink video signal as a digital baseband I/Q data, do the resource mapping, and the OFDM modulation. The video signal is then transmitted through the optical link using the green laser diode into the underwater channel.

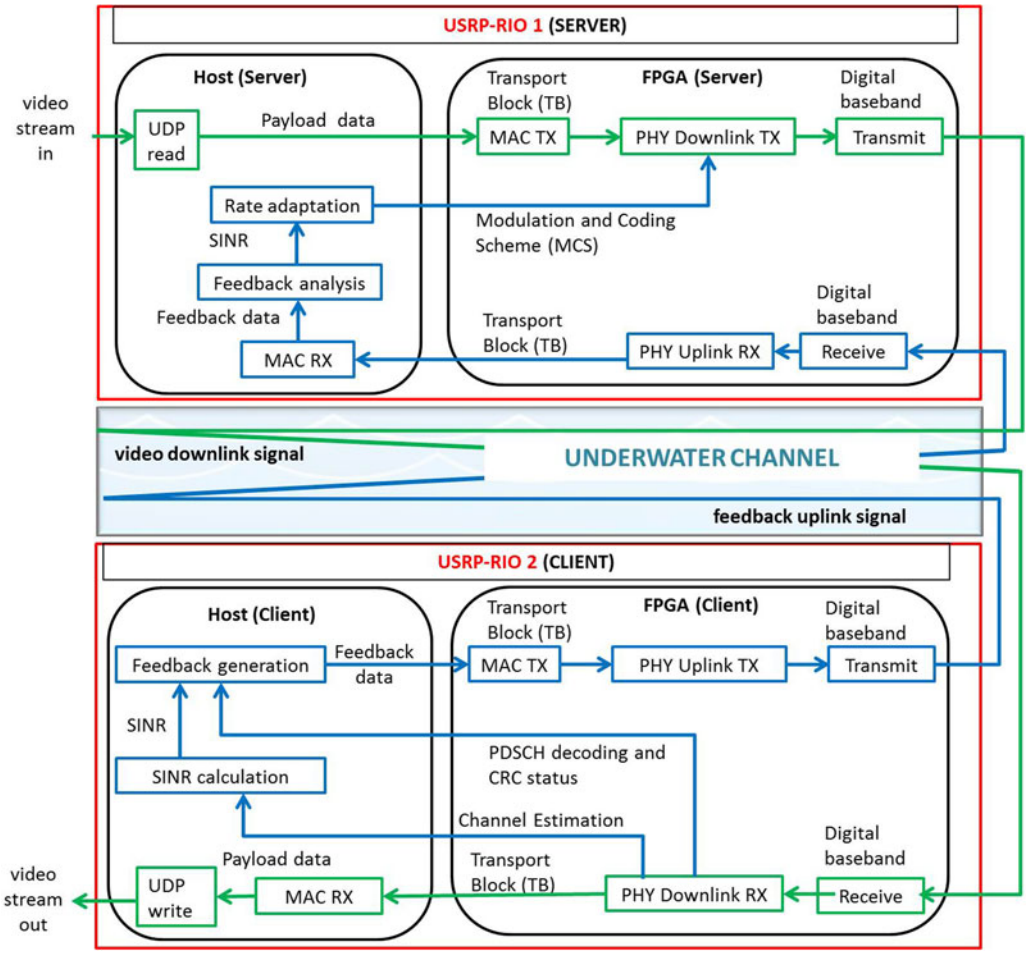

Fig. 1. Block diagram of the system.

2.2 Downlink Receiver Module

When the video signal is received at the second USRP-RIO (Client) at the physical layer of the downlink receiver denoted as (PHY downlink RX), it gets demodulated and decoded at the physical channels. This involves also processing of the primary synchronization sequence (PSS) based synchronization, the demodulation of the OFDM, the resources de-mapping, the channel estimation and equalization, the decoding of the control channel PDCCH, and the decoding of the downlink data shared channel PDSCH. It will then be followed by disassembling of the transport block TB and extracting the payload bytes at the MAC RX. Finally, this payload data is written to a UDP socket using the (UDP write) command. The video data can then be displayed by the external application and processed by the host PC.

2.3 Uplink Transmitter Module

In the uplink, in order to provide the feedback on the channel and reception status to the first USRP-RIO (Server), the channel estimation that was done on the PHY downlink RX at the FPGA (Client) will be fed into the Host (Client) application to calculate the signal-to-interference-noise-ratio (SINR). The SINR is based on the channel estimation used for PDSCH decoding and using cell-specific reference signals (CRS). The feedback generation process creates a message for the measured SINR and the ACK/NACK information which is the Cyclic Redundancy Check (CRC) results of the PDSCH decoding of the previously received video frame.

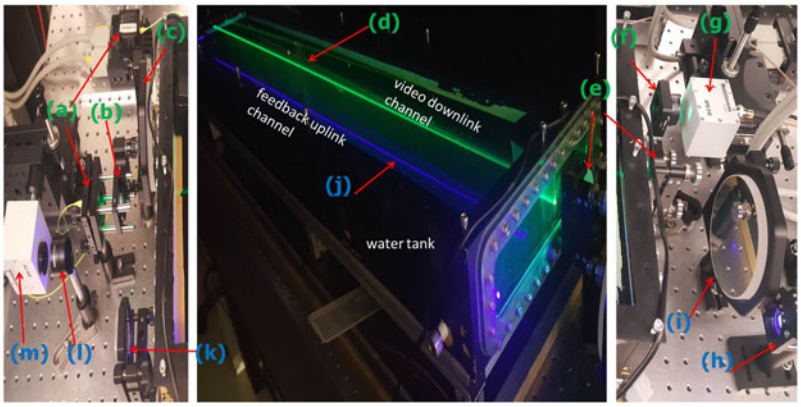

Fig. 2. Actual photograph of the water tank showing: Downlink Channel (a) Green laser and driver mount, (b) collimator lens, (c) mirror, (d) green laser beams underwater, (e) mirror, (f) focusing lens, (g) avalanche photodiode (APD), and Uplink Channel (h) Blue laser and collimator lens, (i) mirror, (j) blue laser beams underwater, (k) mirror, (l) focusing lens, (m) avalanche photodiode (APD).

The physical layer of the uplink transmitter denoted as (PHY uplink TX) will perform a similar role as that of the (Server), but in the uplink direction. It will encode the physical channels and create the uplink signal as digital baseband I/Q data. It will also encode the uplink data shared channel (PUSCH), perform the resource mapping, and do the OFDM modulation. The feedback signal is then transmitted through the optical link using the blue laser diode into the underwater channel.

2.4 Uplink Receiver Module

When the feedback signal is received at the first USRP-RIO (Server) at the physical layer of the uplink receiver denoted as (PHY uplink RX), it gets demodulated and decoded at the physical channels. This includes OFDM demodulation, resource de-mapping, channel estimation and equalization, and decoding of the physical uplink data shared channel (PUSCH). At the feedback analysis stage the SINR and the ACK/NACK information will be fetched from the feedback message.

The subsequent process is to perform the throughput rate adaptation by adjusting the modulation and coding scheme (MCS) based on the measured and reported SINR in order to minimize the block error rate (BLER) of the PDSCH decoding. This will close the feedback loop and pass the new and improved settings to the PHY downlink TX at the start of the new session of underwater UHD video transmission.

3. Hardware Experimental Setup

The actual photograph of the bi-directional underwater UHD video transmission system setup is shown in Fig. 2, while Fig. 3 shows the system's hardware block diagram. We utilized two distinctive wavelengths to avoid any inter-symbol interference (ISI) that can result from locating two adjacent beams with wavelengths relatively within proximity from each others. Maalox solution was added based on [21], to simulate different water turbidity, while the estimated attenuation coefficient of the water we used is based on [22]. Table 1 shows he absorption and scattering coefficients corresponding to the clear ocean and harbor II water types and the added amount of Maalox.

3.1 Downlink Optics Setup

The detailed specifications of the optics system setup are summarized for downlink channel in Table 2. We utilize a 15 mW commercially available, TO-9 packaged and single-mode fiber-pigtailed green LD (Thorlabs LP520-SF15) as the optical transmitter for the downlink video streaming

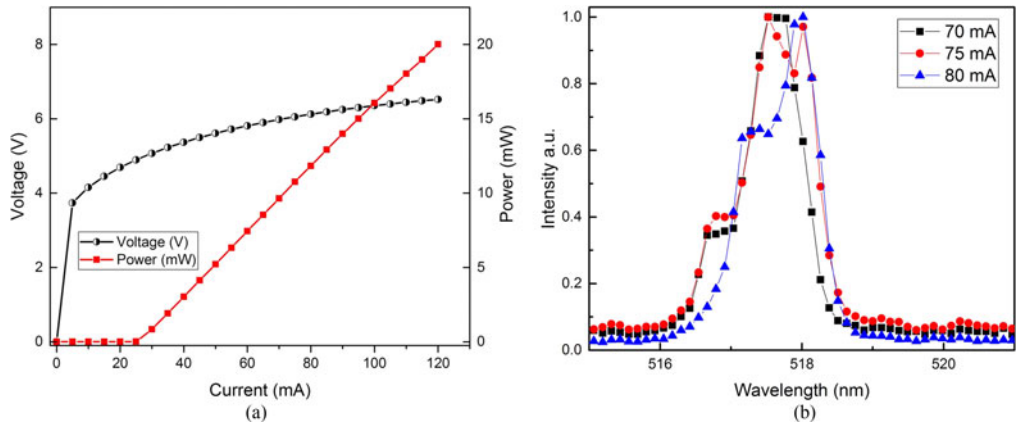

Fig. 3. Schematics of the bi-directional underwater video transmission system with feedback over a reconfigurable wireless optical link.

TABLE I

Representative Absorption, Scattering and Total Attenuation Coefficients and Maalox Volume

Water Type	a (m^{-1})	b (m^{-1})	c (m^{-1})	V(μL)
Clear ocean	0.114	0.037	0.151	77.1
Harbor II	0.366	1.824	2.19	1118.7

TABLE II

Specifications of the Downlink Channel Photonics Setup

Optical Device	Details	Description	Value
Green laser diode	Thorlabs LP520-SF15	Optical output power	15mW
		Full-width at half-maximum	1.0 nm
		Threshold current	28 mA
		Slope efficiency	3.1%
		Emission center wavelength at 70 mA	517.6 nm
Laser driver mount	Thorlabs LDM9LP		
Collimator lens	Thorlabs LA1027-A	Plano-convex lens	
		Diameter	25.4 mm
		Focal length	35 mm
Underwater tank	Material: Polyvinyl Chloride (PVC)	Dimensions	1.5x2.7x0.63 m^3
	Estimated attenuation coefficient		0.071 m^{-1}
Avalanche photodiode	Menlo Systems APD210	Cut-off bandwidth	1 GHz
		Active diameter	0.5 mm
		Noise equivalent power	0.4 $pW/Hz^{1/2}$
		Responsivity at 520 nm	13 A/W
Focus lens	Thorlabs LA1951-A	Focal length	25.4 mm

channel. We show in Fig. 4 (a) the light-current-voltage (L-I-V) curves, and in (b) the emission spectra of the green LD.

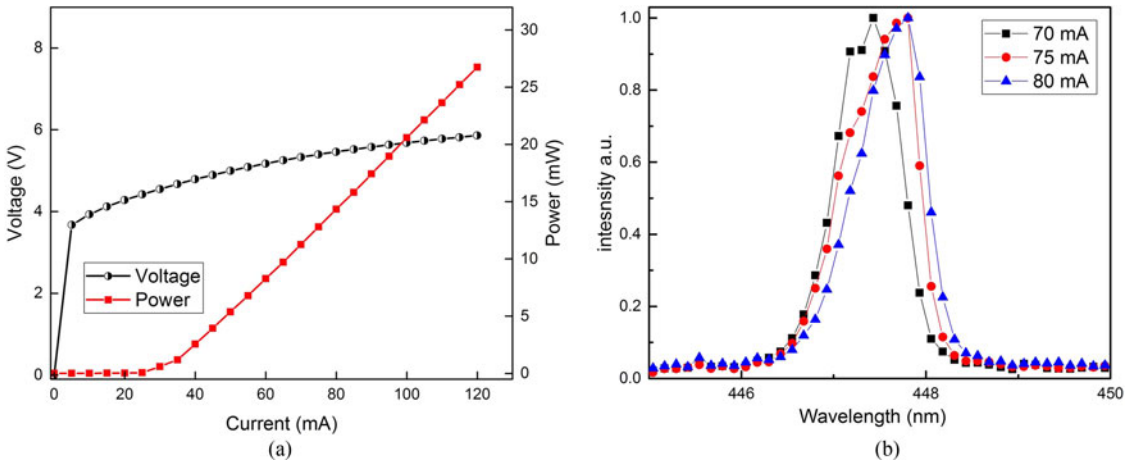

Fig. 4. The 520 nm LD characteristics at 25 °C: (a) L-I-V curves, threshold current (28 mA), slope efficiency ≈3.1% (b) optical spectra with increasing bias currents.

TABLE III
Specifications of the Uplink Channel Photonics Setup

Optical Device	Details	Description	Value
Blue laser diode	Thorlabs LP450-SF15	Optical output power	15mW
		Full-width at half-maximum	0.9 nm
		Threshold current	32 mA
		Slope efficiency	4.8%
		Emission center wavelength at 70 mA	447.3 nm
Laser driver mount	Thorlabs LDM9LP		
Collimator lens	Thorlabs LA1951-A	Plano-convex lens	
		Diameter	25.4 mm
		Focal length	25.4 mm
Avalanche photodiode	Menlo Systems APD210	Cut-off bandwidth	1 GHz
		Active diameter	0.5 mm
		Noise equivalent power	0.4 pW/Hz$^{1/2}$
		Responsivity at 450 nm	5 A/W
Focus lens	Thorlabs LB1761	Focal length	25.4 mm

3.2 Uplink Optics Setup

The uplink channel utilizes another 15 mW commercially available, TO-9 packaged and single-mode fiber-pigtailed blue LD (Thorlabs LP450-SF15) as the optical transmitter for the feedback control channel. The detailed specifications of the optics system setup are summarized for the uplink channel in Table 3. Fig. 5 (a) presents the light-current-voltage (L-I-V) curves of the pigtailed blue LD, and in (b) the emission spectra.

3.3 OFDM Implementation

The physical channels and signals implemented in our framework used OFDM modulation to maximize the bandwidth utilization (bits/s/Hz), and are in general complying with the specifications in [23]–[25]. Prior to the generation of the OFDM signals, initially the input data bit sequence

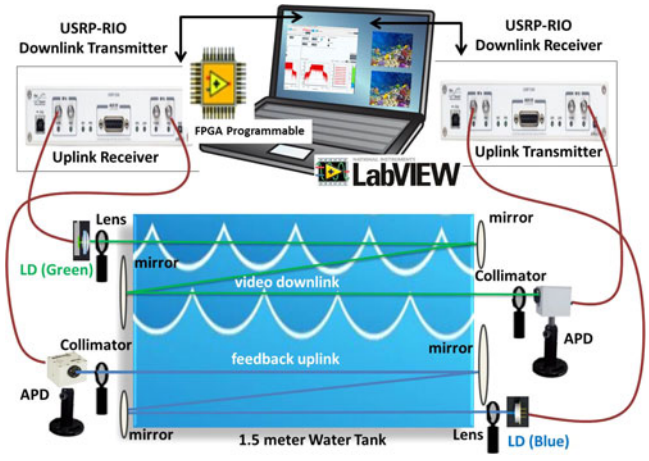

Fig. 5. Characteristics of the 450 nm LD at 25 °C: (a) L-I-V curves, threshold current (32 mA), slope efficiency ≈4.8% (b) optical spectra with increasing bias currents.

is converted from serial into parallel (S/P), encoded and mapped into QAM symbols. This output sequence of complex waveforms from the constellation mapping form a vector input to the 2,048-point Inverse Fast Fourier Transform (IFFT) to form the OFDM signals, making 2,048 subcarriers per OFDM symbol in the frequency-domain. After that, a conversion from parallel to serial (P/S) is performed before the insertion of the Cyclic Prefix (CP), which is enabled in normal mode with length of 166 for symbol 0, and 144 for symbols from 1 to 6. The CP helps to suppress the link ISI. Following a digital-to-analog conversion (DAC), the QAM-OFDM signals are superimposed on the built-in Bias-tee within the laser diode mount to directly modulate the LD. After the signal is transmitted through the underwater channel, at the receiver side the inverse processes are performed; ADC, the removal of CP, S/P, the FFT to convert to frequency-domain subcarriers and for demapping back to QAM symbols, and finally P/S conversion. The OFDM parameters configuration comprise of 15khz of subcarrier spacing when normal cyclic prefix setup is used. Each transmission frame is 10 ms long and is made up of 10 subframes with length of 1 ms. This comprises 30,720 complex time domain baseband samples at a rate of 30.72 MS/s. Each subframe is divided into 14 OFDM symbols, with symbol duration of (2048 multiples of the sampling period). Out of the 2,048 subcarriers there are 1,200 subcarriers used for the transmission and organized in sets of 12 tsubcarriers to form 100 physical resource blocks (PRBs) and there are 7 OFDM symbols per RBE.

4. Experimental Results and Discussions

In this section, we present our experimental results as follows: visual analysis, throughput analysis and finally we discuss received video quality using PSNR analysis. Throughout this discussion we will present quantitative measures to show the advantages and the tradeoffs of using higher orders of modulations in different underwater channels. We will discuss the system's performance when higher resolutions of video quality are transmitted.

4.1 Visual Analysis

We start with analyzing the visual influences and aspects of the performance. Fig. 6 shows the constellation graphs for harbor II water when the UHD video, with 4K resolution of 4096 x 1762, and audio track are transmitted over the downlink channel while using 64-QAM, 16-QAM, and QPSK modulations, as in (a), (b), and (c) respectively. The sub-figure (d) shows the QPSK modulation scheme for the uplink feedback channel. We observe that the constellation graphs are distinguishable. In Fig. 7, we provide snap shots with very clear details and bright colors of the

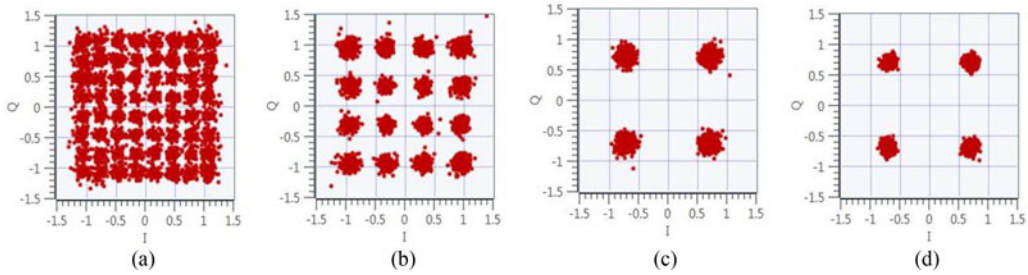

Fig. 6. Constellation graph harbor II water: (a) 64-QAM, (b) 16-QAM, (c) QPSK, (d) feedback QPSK.

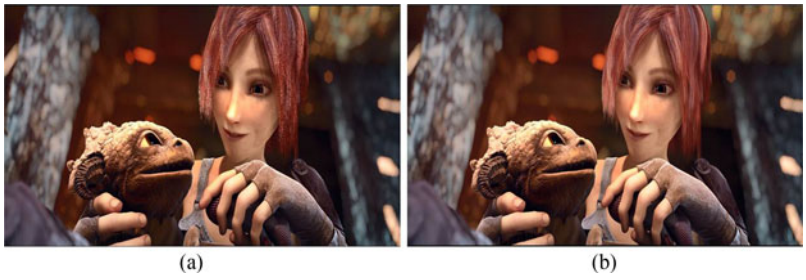

Fig. 7. Video snapshot, harbor II water, 64-QAM, 4K resolution: (a) transmitted video, (b) received video.

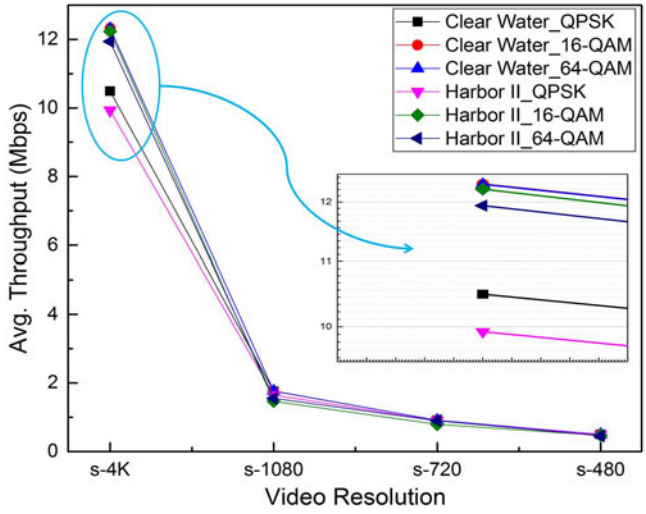

Fig. 8. Average throughput versus video resolution.

(a) transmitted and (b) received UHD video when using 64-QAM modulation scheme and in harbor II water type.

4.2 Throughput Analysis

In the following, we present the video transmission throughput analysis. In Fig. 8, we show the measured average throughput against video resolutions when different streams are transmitted in different water types and using different modulation schemes. We use the following verified resolutions: 4096 (4K UHD), 1080 (HD), 720, and 480 for the same video stream.

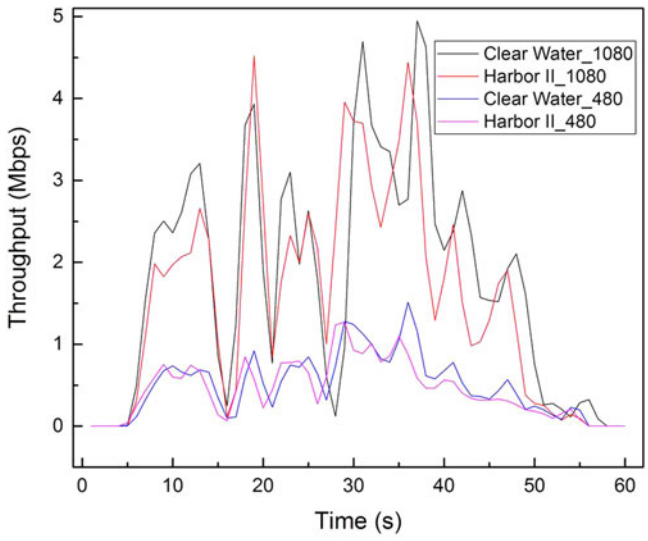

Fig. 9. Throughput over time for the 1080 and 480 video resolutions.

It is apparent that the average throughput decreases when decreasing the video quality. In addition, it is interesting to note that our experiment verified that the throughput was not only decreasing while the water turbidity increases when going from clear ocean to harbor II water type, but also that the modulation scheme effects the video transmission throughput when the 4K UHD video is sent more than the other lower resolutions. From the graph, we zoomed into the 4K UHD video throughput area and found that the average throughput is the lowest when using QPSK in harbor II water. The second lowest is while using QPSK in clear ocean. While comparing 64-QAM and 16-QAM, an interesting finding is that the latter outperformed the 64-QAM modulation in harbor II water, and the 16-QAM performance was not heavily affected by the water turbidity.

When transmitting UHD video in clear ocean, the 16-QAM and 64-QAM modulations are relatively in close proximity. This is suggesting there are tradeoffs between the spectral efficiency gained by the 64-QAM scheme and its throughput performance, and the tradeoff becomes apparent in all aspects of performance as we increase the video quality (resolution) as we just noticed and will again realize that tradeoff in the following set of figures. Using OFDM with higher orders of modulations such as 64-QAM, although it facilitates increasing the bandwidth per symbol, it makes the selectivity of individual subcarrier frequencies much harder in such a noisy channel.

We show in Fig. 9, the throughput variations over time for video streams with the resolutions of 1080 and 480 in clear ocean and harbor II water types, while the modulation scheme is set to 64-QAM. Interestingly enough that the patterns of the throughput trace are matching, however the comparison suggests that the effects are more for the higher resolution. This is in agreement with our previous findings in Fig. 8.

We now examine, in more details, the throughput of the 4K UHD video streams when transmitted in harbor II water type. Fig. 10 shows the throughput over the whole video time (about 15 minutes), under different modulation schemes, 16-QAM in (a) and 64-QAM in (b) of Fig. 10. These two figures show the similarity of both throughput spectrums. However, we clearly notice the QPSK in (c) is clipped at the maximum rate it can support (around 15 Mbps), while this agrees with the throughput shape and pattern in clear ocean as in (d) when QPSK is used.

In Fig. 11, we closely examine the throughput of the 4K UHD video transmission in harbor II water type to help us compare the performance of the different modulation schemes. Part (a) shows the three schemes QPSK, 16-QAM, and 64-QAM altogether and overlapping except where QPSK is clipped as we explained earlier in Fig. 10. It can be also noticed that 16-QAM is the highest throughput. In order to clearly show this, we zoomed into a portion of the throughput graph in part (b) of the figure.

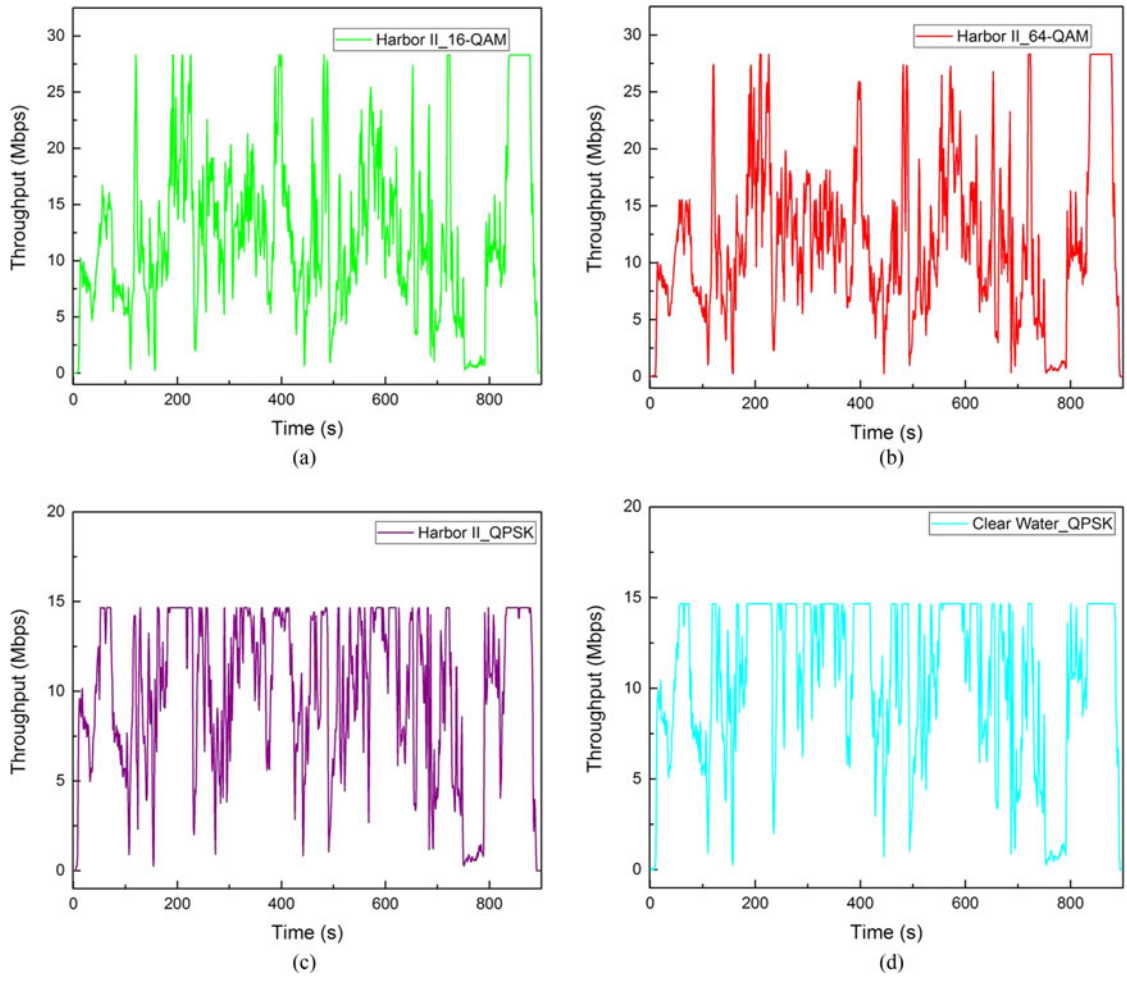

Fig. 10. Throughput over time for the 4K UHD video resolution in harbor II water using: (a) 16-QAM, (b) 64-QAM, (c) QPSK, and in (d) clear ocean using QPSK.

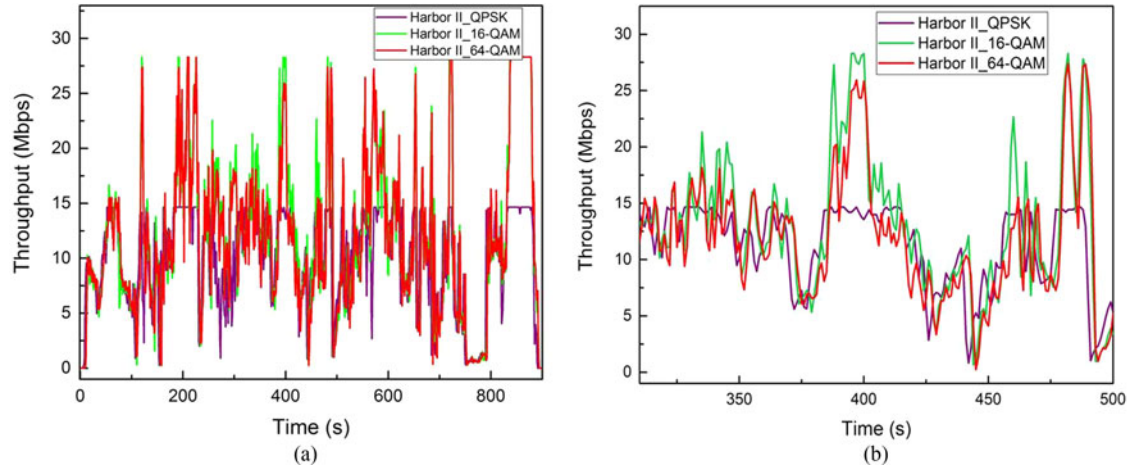

Fig. 11. Throughput over time for the 4K video resolutions in harbor II water for QPSK, 16-QAM, and 64-QAM: (a) 15 minutes (b) zooming into 3 minutes only.

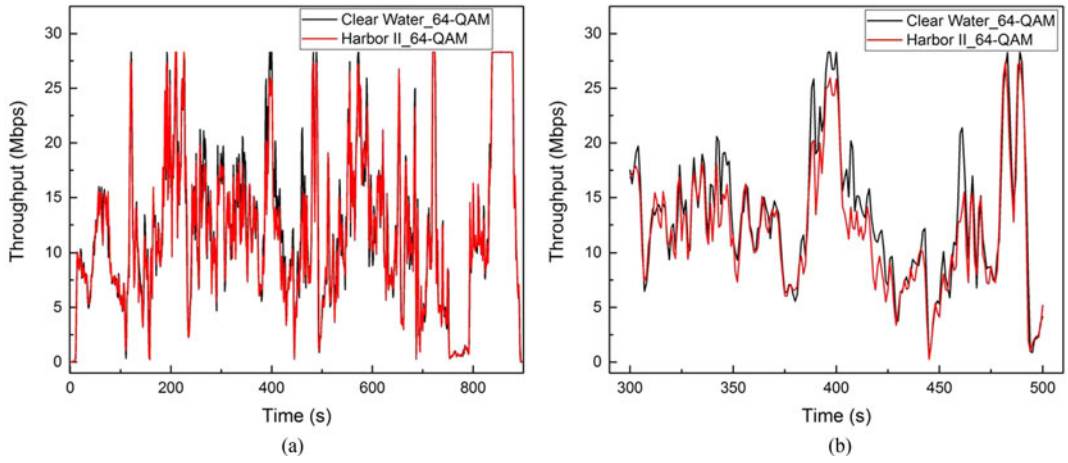

Fig. 12. Throughput over time for the 4K video resolutions using 64-QAM in clear ocean and harbor II: (a) 15 minutes (b) zooming into 3 minutes only.

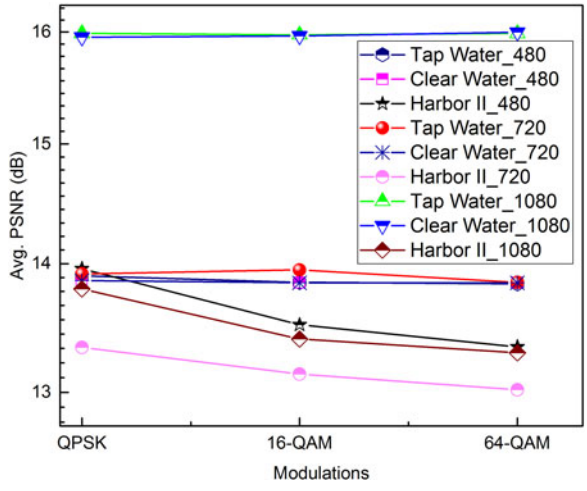

Fig. 13. Average PSNR for video resolutions 480, 720, and 1080 versus modulations in all water types.

Finally, we show in Fig. 12 the comparison of the performance of the 64-QAM modulation scheme for the 4K UHD video streams when sent into the clear ocean against the harbor II. Part (a) shows the throughput for the whole time of the video and (b) for only 3 minutes to easily recognize the difference. It shows that the throughput is lower in harbor II water. However, it is important to mention that the throughput traces are very closely matching which proofs that the performance of the system is stable even under the most turbid water conditions (harbor II), and matches that of the clear ocean although considering that the video streams are in UHD resolution.

4.3 PSNR Analysis

In the last part of this analysis, we discuss the effects of using different modulation schemes on UHD video transmission quality in the most turbid harbor II water. We use Peak-Signal-to-Noise-Ratio (PSNR) in our analysis to show the difference between the transmitted and received video streams. As we show in Fig. 13, we consider the resolution of the video streams to be 480, 720 and 1080. It is apparent that 1080 is the highest average PSNR among all the resolutions, at the top of the figure, and there is no difference between transmitting in the tap water and clear ocean.

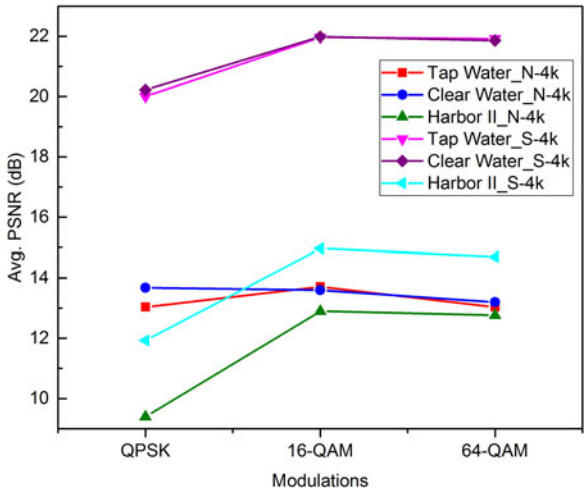

Fig. 14. Average PSNR for 4K UHD video resolutions versus modulations in all water types.

While also noticing that the average PSNR will drop down when we transmit the video in harbor II water type. There is no apparent difference between the three modulations schemes QPSK, 16-QAM and 64-QAM when transmitting in tap water and clear ocean. However, an interesting finding is that the 64-QAM produces the least average PSNR when transmitting those resolutions.

The results presented in Fig. 14 show the effects of using different modulation techniques on transmitting 4K UHD video in channels with different water turbidity levels. Tap water and clear ocean do not present remarkable differences when using different modulations, while in harbor II it presents clear evidence that the QPSK will provide the least average PSNR. On the other hand, in harbor II, the results do not show big difference between using either 16-QAM or 64-QAM on the video quality.

Hence, although visual analysis would infer that we have a perfect transmission of UHD video in real time, but when we further quantitatively analyse the throughput and PSNR we would become able to suggest the most optimized configurations in choosing the best modulation scheme and video resolution in different water visibility.

5. Conclusion

In this work, we experimentally demonstrated an ultra high definition (UHD) quality and real-time video streaming into an underwater wireless optical communication (UWOC) link up to 4.5 m distance using QPSK, 16-QAM and 64-QAM OFDM modulation schemes in clear ocean and harbor II water types. The communication system is based on bi-directional framework that can transmit the video using downlink channel and receive the feedback control on the uplink channel. The UHD video system utilizes LabVIEW software packages built into USRP-RIO hardware. The video packets are transmitted on the downlink channel which is integrated into the wireless optical transmission link using a commercially available TO-9 packaged pigtailed 520 nm green LD as the transmitter and an APD module as the receiver. The feedback control packets are transmitted on the uplink channel which is integrated into the wireless optical transmission link using a commercially available TO-9 packaged pigtailed 450 nm blue LD as the transmitter and an APD module as the receiver. The UHD and live video transmission has been demonstrated and proven to be reliable resulting in clear constellation points and clear video images. The achieved throughput for streaming UHD video is 15 Mbps for QPSK, and 30 Mbps for both 16-QAM and 64-QAM in harbor II water type. Additionally, the PSNR metric was used to evaluate the quality of the received UHD video. The results values were up to 16 dB for 64-QAM when streaming UHD video in harbor II water and 22 dB in clear ocean water. When our proposed solution is integrated into underwater robotics and

underwater wireless sensor networks, it will enable a new era of ocean discovery and exploration. Collecting research samples for onshore testing and ROVs periodic surfacing is minimized. The underwater life can be inspected, monitored, and repaired as required while keeping it within its natural boundaries.

Acknowledgements

The author would like to thank the KAUST Photonics laboratory for facilitating the use of their devices and providing the necessary support and logistics to complete the experiments.

References

[1] The impact of population momentum on future population growth, United Nations, Dept. Econ. Social Affairs, Population Division, New York, NY, USA, 2017. [Online]. Available: https://esa.un.org/unpd/wpp/Publications/Files/PopFacts_2017-4_Populati on-Momentum.pdf. Accessed on: Feb. 2018.
[2] World population projected to reach 9.7 billion by 2050, United Nations, Dept. Econ. Social Affairs, New York, NY, USA, 2015. [Online]. Available: http://www.un.org/en/development/desa/news/population/2015-report.html. Accessed on: Feb. 2018.
[3] A. Shukla and H. Karki, "Application of robotics in offshore oil and gas industry—A review Part II," *Robot. Auton. Syst.*, vol. 75, pp. 508–524, 2016.
[4] O. Khatib *et al.*, "Ocean one: A robotic avatar for oceanic discovery," *IEEE Robot. Autom. Mag.*, vol. 23, no. 4, pp. 20–29, Dec. 2016.
[5] R. Diamant *et al.*, "On the relationship between the underwater acoustic and optical channels," *IEEE Trans. Wireless Commun.*, vol. 16, no. 12, pp. 8037–8051, Dec. 2017.
[6] J. Xu, "Towards broadband long-reach underwater wireless optical communication," in *Proc. Asia Commun. Photon. Conf.*, 2016, Paper AS1D.1.
[7] C.-Y. Li *et al.*, "16 Gb/s PAM4 UWOC system based on 488-nm LD with light injection and optoelectronic feedback techniques," *Opt. Exp.*, vol. 25, no. 10, pp. 11 598–11 605, May 2017.
[8] W. Tsai-Chen *et al.*, "Blue laser diode enables underwater communication at 12.4 Gbps," *Sci. Rep*, vol. 7, 2017, Art. no. 40480.
[9] H.-H. Lu, *et al.*, "An 8 m/9.6 Gbps underwater wireless optical communication system," *IEEE Photon. J.*, vol. 8, no. 5, Oct. 2016, Art. no. 7906107.
[10] J. Xu *et al.*, "Directly modulated green-light diode-pumped solid-state laser for underwater wireless optical communication," *Opt. Lett.*, vol. 42, no. 9, pp. 1664–1667, May 2017.
[11] Y. Ren *et al.*, "4 Gbit/s underwater transmission using OAM multiplexing and directly modulated green laser," in *Proc. Conf. Lasers Electro-Opt.*, 2016, Paper. SW1F.4.
[12] Y. Chen *et al.*, "26 m/5.5 Gbps air-water optical wireless communication based on an OFDM-modulated 520-nm laser diode," *Opt. Exp.*, vol. 25, no. 13, pp. 14 760–14 765, Jun. 2017.
[13] H. M. Oubei *et al.*, "Wireless optical transmission of 450 nm, 3.2 Gbit/s 16-QAM-OFDM signals over 6.6 m underwater channel," in *Proc. Conf. Lasers Electro-Opt.*, 2016, Paper. SW1F.1.
[14] Z. Vali, A. Gholami, Z. Ghassemlooy, D. G. Michelson, M. Omoomi, and H. Noori, "Modeling turbulence in underwater wireless optical communications based on monte carlo simulation," *J. Opt. Soc. Amer. A*, vol. 34, no. 7, pp. 1187–1193, Jul. 2017.
[15] H. M. Oubei *et al.*, "Simple statistical channel model for weak temperature-induced turbulence in underwater wireless optical communication systems," *Opt. Lett.*, vol. 42, no. 13, pp. 2455–2458, Jul. 2017.
[16] M.-A. Chancey, "Short range underwater communication links," Master thesis, Dept. Elect. Eng., North Carolina State Univ., Raleigh, NC, USA, 2005.
[17] G. -Baiden, and Y. -Bissiri, "High bandwidth optical networking for underwater untethered telerobotic operation," in *Proc. IEEE Oceans*, 2007, pp. 1–9.
[18] M. -Doniec, A. -Xu, and D. -Rus, "Robust real-time underwater digital video streaming using optical communication," in *Proc. IEEE Int. Conf. Robot. Autom.*, 2013, pp. 5117–5124.
[19] M. -Sun, B. -Zheng, L. -Zhao, X. -Zhao, and F. -Kong, "A design of the video transmission based on the underwater laser communication," in *Proc. IEEE 2014 Oceans-St. Johns.*, 2014, pp. 1–4.
[20] A. Al-Halafi, H. M. Oubei, B. S. Ooi, and B. Shihada, "Real-time video transmission over different underwater wireless optical channels using a directly modulated 520 nm laser diode," *J. Opt. Commun. Netw.*, vol. 9, no. 10, pp. 826–832, Oct. 2017.
[21] A. Laux *et al.*, "The abc's of oceanographic lidar predictions: A significant step toward closing the loop between theory and experiment," *J. Mod. Opt.*, vol. 49, no. 3/4, pp. 439–451, 2002.
[22] J. W. Giles and I. N. Bankman, "Underwater optical communications systems. Part 2: Basic design considerations," in *Proc. IEEE Mil. Commun. Conf.*, 2005, vol. 3., pp. 1700–1705.
[23] *Evolved Universal Terrestrial Radio Access (E-UTRA); Physical Channels and Modulation*, 3GPP TS36.211 V 10.7.0 Release 10, Feb. 2013.
[24] *Evolved Universal Terrestrial Radio Access (E-UTRA); Multiplexing and Channel Coding*, 3GPP TS36.212 V10.8.0 Release 10, Jun. 2013.
[25] *Evolved Universal Terrestrial Radio Access (E-UTRA); Physical Layer Procedures*, 3GPP TS36.213 V10.12.0 Release 10, Mar. 2014.